

Perspectives on Compound Flooding in Chinese Estuary Regions

Xu, Hanqing; Ragno, Elisa; Tan, Jinkai; Antonini, Alessandro; Bricker, Jeremy D.; Jonkman, Sebastiaan N.; Liu, Qing; Wang, Jun

10.1007/s13753-023-00482-1

Publication date 2023

Document Version Final published version

Published in

International Journal of Disaster Risk Science

Citation (APA)

Xu, H., Ragno, E., Tan, J., Antonini, A., Bricker, J. D., Jonkman, S. N., Liu, Q., & Wang, J. (2023). Perspectives on Compound Flooding in Chinese Estuary Regions. *International Journal of Disaster Risk* Science, 14(2), 269-279. https://doi.org/10.1007/s13753-023-00482-1

Important note

To cite this publication, please use the final published version (if applicable). Please check the document version above.

Other than for strictly personal use, it is not permitted to download, forward or distribute the text or part of it, without the consent of the author(s) and/or copyright holder(s), unless the work is under an open content license such as Creative Commons.

Takedown policy
Please contact us and provide details if you believe this document breaches copyrights. We will remove access to the work immediately and investigate your claim.

ARTICLE



Perspectives on Compound Flooding in Chinese Estuary Regions

 $Hanqing Xu^{1,2} \cdot Elisa Ragno^2 \cdot Jinkai Tan^3 \cdot Alessandro Antonini^2 \cdot Jeremy D. Bricker^{2,4} \cdot Sebastiaan N. Jonkman^2 \cdot Qing Liu^1 \cdot Jun Wang^1$

Accepted: 15 March 2023 / Published online: 11 April 2023 © The Author(s) 2023

Abstract

Extreme surges and rainfall represent major driving factors for compound flooding in estuary regions along the Chinese coast. The combined effect of extreme surges and rainfall (that is, compound floods) might lead to greater impacts than if the drivers occurred in isolation. Hence, understanding the frequency and severity of compound flooding is important for improving flood hazard assessment and compound flood resilience in coastal cities. In this study, we examined the dependence between extreme surges and corresponding rainfall events in 26 catchments along the Chinese coastline during typhoon and non-typhoon seasons using copula functions, to identify where the two drivers more often occur together and the implication for flood management in these locations. We found that the interaction between flood drivers is statistically significant in 10 catchments located around Hainan Island (south) and Shanghai, where surge peaks occur mainly during the typhoon season and around the Bohai Sea (north), where surge peaks occur mainly during the non-typhoon season. We further applied the copula-based framework to model the dependence between surge peaks and associated rainfall and estimate their joint and conditional probability in two specific locations—Hainan Island and the Bohai Sea, where the correlation between flood drivers is statistically significant. We observed that in Hainan Island where most of the surge peaks occur during the typhoon season, extreme rainfall events during the typhoon season are generally more intense compared to annual maxima rainfall. In contrast, around the Bohai Sea where surge peaks occur mainly outside the typhoon season, rainfall is less intense than annual maxima rainfall. These results show that the interaction between extreme surges and rainfall can provide valuable insight when designing coastal and urban infrastructure, especially in highly populated urban areas prone to both coastal and pluvial flooding, such as many Chinese coastal cities.

Keywords China · Coastal catchments · Compound flooding · Copula function · Extreme surge · Optimal threshold

- Hanqing Xu H.Xu-4@tudelft.nl
- ⊠ Elisa Ragno E.Ragno@tudelft.nl
- ¹ Institute of Eco-Chongming (IEC), Key Laboratory of Geographic Information Science of Ministry of Education and School of Geographic Sciences, East China Normal University, Shanghai 200241, China
- Faculty of Civil Engineering and Geosciences, Delft University of Technology, 2628 CN Delft, The Netherlands
- ³ School of Atmospheric Sciences and Key Laboratory of Tropical Atmosphere-Ocean System of Ministry of Education, Sun Yat-sen University, Zhuhai 519082, China
- Department of Civil and Environmental Engineering, University of Michigan, Ann Arbor, MI 48109, USA

1 Introduction

Around 70% of the Chinese coastline is lower than 3 m above sea level (a.s.l.), making it extremely sensitive to coastal flooding (Shi et al. 2020). In estuary regions, the interactions of multiple flood drivers, such as local rainfall, wave effects, tidal amplitude, and surge-tide interactions can exacerbate the probability of flooding, causing great economic losses and casualties (Saleh et al. 2017; Vousdoukas et al. 2018; Fang, Wahl, Fang et al. 2021). In the literature, flood events generated by the interaction between multiple physical drivers, which might not be extremes if considered in isolation, are referred to as compound flood events (Couasnon et al. 2020).

In China, high storm surges and extreme rainfall during the typhoon season are the major driving factors of flooding along the coast (Wu et al. 2021; Liu et al. 2022). Typhoons

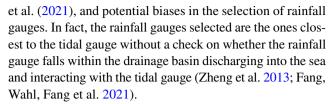


may produce strong onshore winds and an inverse barometric effect, which result in extreme surges, while simultaneously produce large quantities of rainfall over land, generating surface runoff. Moreover, high sea levels can prevent the normal discharge of surface runoff due to rainfall excesses, potentially leading to backwater effects along rivers and increasing the probability of compound flooding (Kossin 2018; Ward et al. 2018).

China is one of the few countries in the world that are affected not only by tropical but also extra-tropical surges (Shi et al. 2015). Typhoon surges usually hit the South China Sea and the East China Sea coast with the characteristics of strong wind speeds, low atmospheric pressure, intense rainfall, large waves and storm surges, and thus strong destructive power (Day et al. 2018; Xiang et al. 2021). Many storms in the Yellow Sea and the Bohai Sea coast usually occur in the spring and autumn (Fang et al. 2016). For example, the combined effect of rainfall and storm tides during Typhoon Winnie (TC9711) in southeastern China killed 342 people and caused a direct economic loss of USD 4.3 billion (State Oceanic Administration 1998). Also, severe flooding due to the combination of surge and rainfall during super typhoon Hato killed at least 12 people in Macau in 2017 (Wang et al. 2019). These examples emphasize the importance of studying the combination of surge and rainfall in estuaries and coastal regions (Zheng et al. 2013; Wahl et al. 2015) to avoid misrepresentations of the flood hazard and improve the resilience of coastal systems (Wahl et al. 2015; Ghanbari et al. 2021).

The relationship between rainfall and surge in estuary regions can have a substantial impact on coastal flood management, despite being challenging to detect from observations as the correlation between observed variables may not be significant (Sadegh et al. 2018; Bevacqua et al. 2020). Most of the available studies on compound flooding investigate locations in the United States and Europe, where tide gauges are densely distributed and provide more than 50 years of observed data (Wahl et al. 2015; Bevacqua et al. 2017; Bevacqua et al. 2019). For example, Wahl et al. (2015) examined the dependence between precipitation and storm surge and reported an increase in compound flood risk during the past decades along the east coast of the United States. According to Zheng et al. (2013), precipitation and storm surge are significantly correlated in the coastal regions of Australia.

Although studies on compound coastal flooding in estuary locations across China are still scarce, recent work by Fang, Wahl, Fang et al. (2021) showed that there is a positive dependence between rainfall and storm surge, especially during the typhoon season, calling for a more in-depth investigation of compound flooding. The current studies have limitations, such as small sample sizes of observations, for example, the 23-year sample in Fang, Wahl, Fang



Hence, this study aimed to improve the current modeling of compound flooding in estuary regions along the Chinese coastline. This is done by analyzing longer records of rainfall (around 36 years) and to carefully select the rainfall gauges to be representative of the inland water received by drainage basins discharging directly into the sea. Moreover, this study aimed to propose guidelines to derive design values for coastal infrastructure in relation to the season in which most of the pairs of surge and corresponding rainfall occur.

Specifically, in this study we first developed a copulabased framework to model the dependence between surge and rainfall, in which rainfall was used as a proxy of the amount of inland water discharged into the sea. Then, we implemented such a framework to derive information on expected rainfall as a function of the magnitude of the surge event in cases where the interaction between surge and rainfall cannot be neglected, that is, where statistically significant correlation exists. Finally, we discuss the implication of this approach for reducing the risk of urban pluvial flooding and increase urban flood resilience in the season in which most of the surge peaks in a specific estuary region occur. The rest of the article is structured as follows. Section 2 provides details of the dataset and study region. Section 3 presents the copula-based framework. Section 4 contains the results of the analysis. Section 5 discusses the advantages and limitations of this work. Finally, Sect. 6 provides a summary of the study.

2 Data and Study Area

In this study, we are interested in estuary regions along the Chinese coast and prone to compound flooding generated by the interaction between rainfall and storm surge. For this reason, the following datasets are selected:

- Catchment Shapefiles. HydroSHEDS database developed by the WWF-US (Fig. 1) (Lehner et al. 2008) to retrieve catchment boundaries.
- (2) Rainfall. Daily rainfall (24h cumulative rainfall) time series gauges managed by the China Meteorological Administration (CMA)¹ and covering the period between 1979 and 2014.



http://data.cma.cn

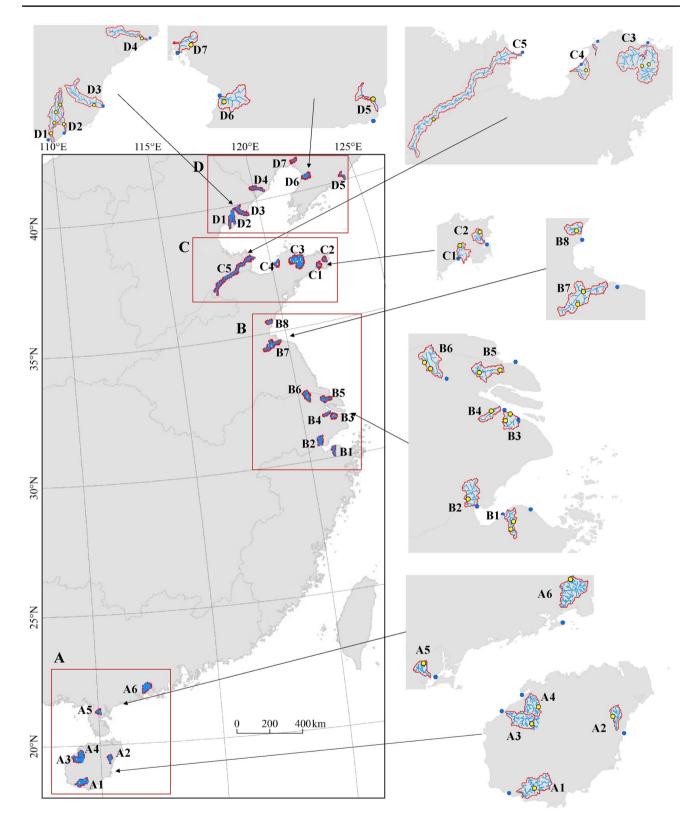


Fig. 1 Location and area of 26 catchments along the Chinese coastline (blue dots represent tide gauges and yellow dots represent rainfall gauges). Label $\bf A$ refers to the region in southern China with a latitude of lower than 21.5°. Catchments labeled as $\bf B$ are located on the east-

ern coast of China, with latitudes ranging from 30 to 37°. Catchments labeled as $\bf C$ are located to the south of the Bohai Sea, with latitudes ranging from 37 to 38°. Finally, catchments labeled as $\bf D$ are located in northern China, with latitudes higher than 38°



Storm Surge. Surge reanalysis data from the Global (3) Tide and Surge Reanalysis (GTSR)² dataset. The GTSR dataset is the first global reanalysis dataset of surges and extreme sea levels, and it is based on hydrodynamic modeling (Muis et al. 2016). The GTSR covers the entire world's coastline and provides near-coast time series of surges and tides from the Dynamic Interactive Vulnerability Assessment model in 1979–2014. The surge was simulated by forcing the global tide and surge model with wind and pressure fields from ERA-Interim. Numerical simulations were carried out at a 10-min temporal resolution. Regarding the application of GTSR/ERA-Interim for surge during typhoon season, the GTSR produced sufficient surge results and is widely used in the East Asian region (Mori et al. 2019).

2.1 Catchment Selection and Description

Since we are interested in estuary regions along the Chinese coast prone to coastal flooding, we need to select estuary locations for which catchment information, surge, and rainfall data are available. Hence, we simultaneously looked at the relative locations of catchment boundaries, rainfall gauges, and surge data. Then, we selected catchments discharging directly into the sea for which at least one rain gauge within the catchment boundary and one surge station in the vicinity of the catchment outlet could be found. Following this approach, we identified 26 hydrological catchments across the entire Chinese coastline (Fig. 1).

The selected catchments across the coastline have lengths up to 100 km and areas up to 1000 km², except catchment C5 that has a length of ~224 km and an area of ~2876 km² (Fig. 2a and Fig. 2b). China's coastline covers approximately 14,500 km and a range of climates. The average annual temperature in the catchments ranges from 10.3 °C (north) to 24.8 °C (south) (Fig. 2c). Figure 2d shows that annual rainfall across the 26 catchments ranges from 575.6 mm (north) to 2183.5 mm (south). For those catchments containing more than one rainfall gauge (8 among the 26 selected), the weighted average of the station rainfall was considered. The weight was estimated based on the distance to the catchment outlet. More specifically, the closest gauge has the highest weight. A small variability between rainfall peaks of stations in the same catchments is observed.

2.2 Pairs of Surges and Rainfall

To develop the copula-based framework, we constructed a dataset of pairs of surge peaks and corresponding rainfall potentially leading to compound flooding. First, we sampled surge peaks from the daily surge reanalysis data following

² https://data.4tu.nl/



the peak-over-threshold approach. To ensure independence between peaks, only peaks spaced at least three days apart were considered (Feng et al. 2018). Then, we ran a preliminary analysis on the correlation between surge peaks and accumulated rainfall over a window of time ranging from the day of the occurrence of the peak to seven days prior to it to investigate the lead time in the response of the catchments to a rainfall event. Based on this analysis, we selected the daily rainfall recorded on the day of the occurrence of the surge peak as the rainfall event, since this combination of surge peak and corresponding rainfall gives the highest correlation for most of the catchments. These pairs of surge and corresponding rainfall were then used to determine a copula-based framework for compound flooding.

3 Methods

A copula-based framework was used to model the dependence between flood drivers. To quantify the probability of the compound hazard generated by the interaction between surge and rainfall, we first evaluated the marginal distributions of surge peaks and corresponding rainfall. Then, we selected a copula function to evaluate the probability of compound flooding. Finally, we estimated design values of surge and rainfall via conditional probability.

3.1 Peaks Over a High Threshold

We selected surge peaks following the peak over threshold (POT) approach. According to Pickands III (1975) and Coles et al. (2001), given a random variable X, the excess is $X_{ex} = x - u$, defined above a large enough threshold u. In order to ensure the independence of the excesses, a declustering technique was also implemented to ensure the independence of excesses (Antonini et al. 2019). The threshold u was selected based on the empirical mean residual life (MRL) and dispersion index (DI). The MRL provides a visual diagnostic tool to select the threshold u in which the average mean of X_{ex} is plotted as a function of u. A suitable u was selected where the plot is approximately linear. On the other hand, the DI, being the ratio between the variance and the mean of the yearly occurrence of the peaks, was used to check whether the peaks above a given threshold u are independent and follow a Poisson distribution. The combination of MRL and DI can provide an indication on a suitable u.

³ See supplementary material, Fig. S3 at https://doi.org/10.4121/d993eec7-82de-4771-b5ff-1cd7cfe4611a.v1.

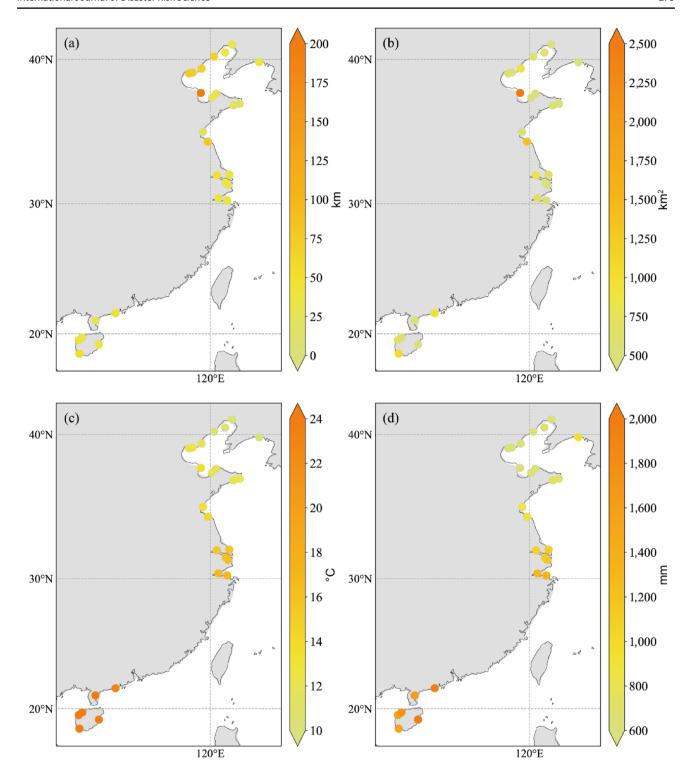


Fig. 2 Catchments investigated in this study. a Catchment length; b Catchment area; c Annual mean temperature; d Annual mean rainfall

3.2 Copula Model

Copula functions have gained popularity in hydrological studies following the work of De Michele and Salvadori (2003). The advantage of copula functions is their ability to

model the dependence between two (or more) random variables independently of their marginal distributions (Sklar 1973). Specifically, given two random variables X and Y with continuous marginal distributions F(x) and G(y), the joint distribution of X and Y is given by



$$F(x,y) = C[F(x), G(y)] = C(u,v)$$
(1)

where C is the copula function and u = F(x) and v = G(y) are uniform margins.

In this study, we restricted our analysis to the most used copulas, namely Gaussian, Clayton, Frank, and Gumbel, as the candidate functions for modeling the joint probability distributions of compound events. This is because they are all one-parameter copulas that can cover different types of dependence behavior, that is, symmetry in the data (Gaussian and Frank copulas) or greater association between variables at the tails, that is, Clayton can capture lower tail dependence and Gumbel upper tail dependence. Moreover, when the sample size of investigated pairs is small, more complex copulas might not provide any advantage. The parameters of each copula function were estimated based on the maximum likelihood estimation (MLE) method (Haseeb 2013). In order to select the copula that best fits the data, the following metrics were considered: the Akaike information criterion (AIC), Bayesian information criterion (BIC), and root mean square error (RMSE).

The AIC and BIC are defined as follows:

$$AIC = -2L(\overline{\vartheta}|y) + 2K \tag{2}$$

$$BIC = -2L(\overline{\vartheta}|y) + Kln(n) \tag{3}$$

where K is the number of estimated parameters in the model including the intercept and $L(\overline{\vartheta}|y)$ is the log-likelihood at its maximum point of the estimated model; n is the sample size. The smaller the AIC and BIC are, the better the fit (Burnham and Anderson 2004).

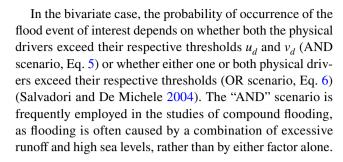
The RMSE is defined as:

$$RMSE = \sqrt{\frac{1}{n} \sum_{i=1}^{n} \left(C_C(u_i, v_i) - C_n(u_i, v_i) \right)^2}$$
 (4)

where n is the number of pairs (u, v); C_C is the theoretical copula; and C_n is the empirical copula. A low RMSE value indicates that the simulated and observed data are close to each other, showing a better accuracy.

3.3 Inferring Design Values via Conditional Probability

A probabilistic dependence model, like copula function, can be used to infer a design value based on the probability of occurrence of the event of interest. When dealing with dependent variables, the (statistical) occurrence of an event, for example, a flood event, is defined in relation to the occurrence of its physical drivers, that is, X and Y (or U and V in the copula domain).



$$P((U > u_d) \cap (V > v_d)) = 1 - u_d - v_d + C(u_d, v_d)$$
 (5)

$$P((U > u_d) \cup (V > v_d)) = 1 + C(u_d, v_d)$$
(6)

For a fixed probability of exceedance, or return period, the pair of variables (u_d, v_d) can be inferred following the "most-likely method," which selects the pair with the highest density, hence the method's name.

However, in some cases, one of the two physical drivers is the most important from a design perspective. For example, higher storm surges, which determine hydraulic loads on coastal and offshore structures, often result from intense typhoons in southeastern China. Higher sea water reduces the discharge capabilities of inland drainage systems, potentially causing pluvial flooding. In such a case, a dependent model can be used to infer the design value of one physical driver, for example, rainfall, when the other one, for example, storm surge, is fixed via conditional probability.

$$P(V > v | U = u_d) = 1 - \frac{\partial C(u, v)}{\partial u}$$
 (7)

4 Results

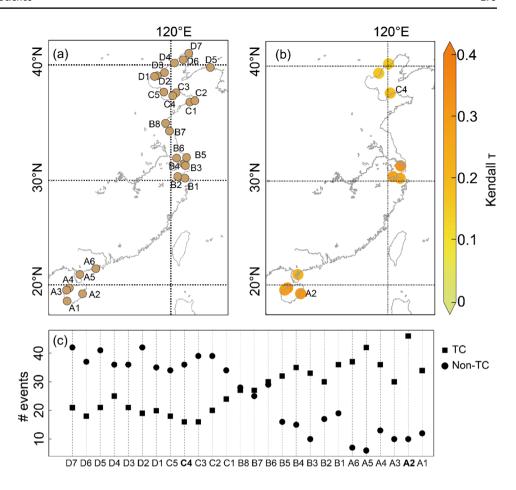
In this section, we examine the dependence between extreme surges and corresponding rainfall events in 26 catchments along the Chinese coastline to identify where the two drivers more often occur together. Our analysis revealed a significant correlation between surge and rainfall in 10 catchments, primarily located in southern and northern China. Then, we implement a copula framework to model the observed dependence and examine changes in the probability of rainfall when conditioned on specific value of storm surge.

4.1 Peaks Selection and Dependence Quantification

We selected surge peaks greater than the thresholds u based on the MRL and DI plots. The thresholds (0.33-1.39 m) in all the catchments range between the 99th and 99.4th percentile of observed surges. The threshold u around Hainan Island is generally lower than other



Fig. 3 a Catchments investigated; b Catchments in which a significant dependence between extreme surge and rainfall was detected; c The occurrence of compound events in the typhoon season and the non-typhoon season. The catchments A2, A3, A4, A5, B1, B2, B3, C4, D3, and D4 exhibit significant correlations between extreme surge and rainfall. The levels of significance of both models emphasize the importance of events during the typhoon season (TC, black square) and the non-typhoon season (Non-TC, black circle). Among these catchments, the bold labels (A2 and C4) indicate those selected for further analysis. Catchment A2 was selected due to the highest occurrence of compound events and significant dependency during the typhoon season. Conversely, catchment C4 exhibits the strongest correlation during non-typhoon season although the number of compound events is not the largest



stations because the western side of Hainan Island (South China), and the mainland across the strait, are sheltered by Hainan Island itself, reducing the surge (Zhang et al. 2017). In addition, the eastern side of Hainan Island has a narrower continental shelf than the rest of the Chinese coast. Surge is proportional to the width of the continental shelf over which the wind blows. In general, a narrow continental shelf results in a smaller surge than a wider shelf. The highest threshold obtained is around Shanghai, at 1.3 m. A declustering time of three days is considered (Feng et al. 2018) to ensure independence between events selected. In the end, we obtained an average of 53 excesses in the 26 catchments over a period of 36 years. The average amount of peaks/pairs is 1.5 per year for all catchments. The maximum number of peaks/pairs is located in catchment D7 and the minimum number of peaks/pairs is in catchment A3. For each excess, we selected the total daily rainfall recorded on the same day to form pairs of surge and rainfall. We quantified the dependence between entire excess pairs of surge peak and rainfall via Kendall's rank correlation coefficient τ significance test (Hauke and Kossowski 2011) (Fig. 3a). We detected a significant correlation (with a level of significance $\alpha = 0.05$) in 10 of the 26 catchments analyzed, especially in southern China

(Fig. 3b). Catchments A2, A3, A4, A5 (south), B1, B2, B3 (center), C4, D3 and D4 (north) show a significant correlation between surge and rainfall (with a level of significance $\alpha = 0.05$). Eastern Hainan Island (catchment A2) shows the highest correlation ($\tau = 0.35$). This is reasonable since Hainan Island is highly affected by typhoons and this implies that extreme surge conditions are often accompanied by high rainfall during typhoon events. We also find statistical dependence between rainfall and surge in three catchments around the Bohai Sea (C4, D3, and D4 gauges, Fig. 3b). Northern China is affected by extratropical storms outside the typhoon season (mainly in the late winter and early spring), which can often cause flooding and damage.

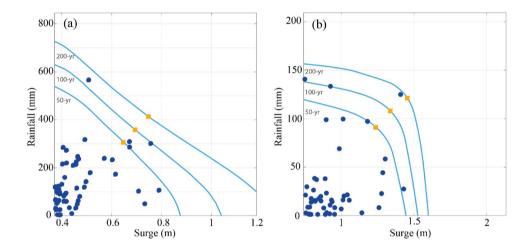
To better understand the influence of seasonality, we count the number of events in the typhoon season (July to October) and the non-typhoon season (November to June of the following year) separately. Figure 3c shows the number of compound events in the typhoon season and the non-typhoon season. After an analysis of the surge peak events, we found that in the south, most of the compound events occur in the typhoon season while in the north, most of the compound events occur during the non-typhoon season.



Table 1 Performance measures of the estimated copula functions

Catchments	Copula type	Max-likelihood	Akaike information criterion (AIC)	Bayesian information criterion (BIC)	Root mean square error (RMSE)
A2	Gaussian	214.8	- 427.6	- 425.6	0.1615
	Clayton	192.7	- 383.4	- 381.4	0.2395
	Frank	223.5	- 445.1	- 443.1	0.1381
	Gumbel	217.5	- 433.1	- 431.1	0.1537
C4	Gaussian	202.5	- 403.1	- 401.1	0.1468
	Clayton	196.3	- 390.6	- 388.6	0.1654
	Frank	206.3	- 410.6	- 408.6	0.1365
	Gumbel	210.5	- 419.1	- 417.1	0.1258

Fig. 4 Isolines of extreme paired data based on the Frank and Gumbel copulas. a Catchment A2; b Catchment C4. The yellow squares show the design values under different joint return periods between the extreme surge and rainfall using the most-likely method



4.2 Selecting the Copula Model

To further analyze the dependence between surge and rainfall and the implication of such dependence on infrastructure design, we focus the following analysis on two locations: Hainan Island (catchment A2) and the Bohai Sea (catchment C4). These locations show positive and significant correlations between storm surge and rainfall. However, in catchment A2 ($\tau = 0.35$) the highest number of surge peaks (46) were observed during typhoon season, while in catchment C4 ($\tau = 0.24$) the highest number of surge peaks were observed during the non-typhoon season (36). Based on the results in terms of AIC, BIC, and RMSE (Table 1), the copulas that best fit the observations are Frank for catchment A2 and Gumbel for catchment C4. Here, empirical margins are assumed.

Following the most-likely approach and based on the "AND" hazard scenario, that is, both rainfall and surge should be above their respective thresholds, Fig. 4 shows the pairs of surge and rainfall corresponding to return periods of 50, 100, and 200 years. The design events (yellow squares in Fig. 4) are given by the point of maximum relative probability density (most-likely method) on the isoline

associated with a fixed return period. The processes of simulating samples from the fitted copulas, estimating the relative likelihood along the isolines, and extracting the most-likely event, was then repeated to determine the three design events associated with the 50, 100, and 200 year return periods. The most extreme observed compound event with rainfall of 123.8 mm and a surge peak of 1.4 m (close to 200 year return period) in Fig. 4b was during typhoon Meari (June 2011). This typhoon caused floods in 17 counties of three provinces on the east coast of China.

4.3 Conditional Design Value of Rainfall

In coastal areas, coastal flooding is driven by sea water level, which depends on both storm surge and astronomical tide. However, sea level might also affect pluvial flooding, since high sea level might prevent inland water discharge by gravity. Hence, we used the dependence model obtained above to assess changes in rainfall probability distribution when information of storm surge is known in relation to the probability distribution of annual maximum rainfall.

From the dependence model (Frank copula for catchment A2 and Gumbel copula for catchment C4) we



Fig. 5 Simulated surges and rainfall under the joint copula model. a Catchment A2; b Catchment C4. The vertical solid line represents the value of the surge at 50 year return period, while the dashed lines represent the range percentiles beside the solid line

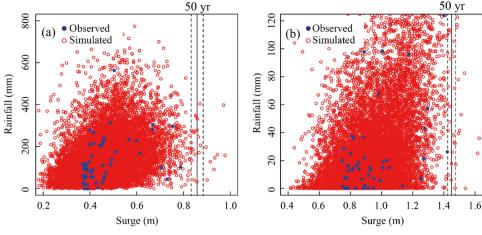
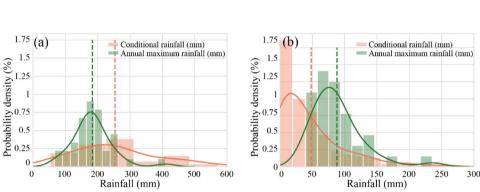


Fig. 6 Comparison of annual maximum rainfall and conditional rainfall at A2 (a) and C4 (b) locations with all the pairs; dashed vertical lines are the median value of rainfall



randomly sampled 10,000 dependent surge and rainfall pairs (red dots in Fig. 5). Then, we selected pairs for which the surge level is close to the 50 year return period event in the univariate case, that is, 0.86 m (0.835–0.885 m) for catchment A2 and 1.45 m (1.425–1.475 m) for catchment C4 (Fig. 5), to obtain the distribution of rainfall conditioned on the 50 year return period surge event.

Figure 6a shows that for catchment A2 (eastern Hainan Island, South China), where the majority of surge peaks occurred during typhoon season, we observe a shift in the rainfall median when rainfall is conditioned on storm surge. Specifically, the median of the rainfall condition on the 50 year return period storm event (258.76 mm/day) is about 40.8% higher than the median of annual maxima rainfall (183.69 mm/day). This result implies that extreme rainfall events during typhoon season are generally more intense compared to most annual maxima events, requiring extra attention when developing a flood protection intervention. For catchment C4 (the Bohai Sea, North China), where the majority of surge peaks occurred outside the typhoon season, we observe the opposite behavior: the median rainfall event conditioned on the 50 year return period surge event (49.43 mm/day) is smaller than the median of the annual maxima rainfall event (88.15 mm/ day).

5 Discussion

Highly urbanized centers such as Chinese coastal cities are prone to flooding from the combined occurrence of surge peaks and high rainfall events. Hence, we investigated the degree of dependence between surge peaks and corresponding rainfall events and its implication in terms of infrastructure design accounting for the seasonality of the surge peak occurrence.

Even though the GTSR dataset used in this study might underestimate surges during typhoon events (Muis et al. 2016; Muis et al. 2017), other studies proved that the use of the GTSR dataset in East Asia is possible and the results are plausible (Mori et al. 2019; Fang, Wahl, Zhang et al. 2021). Moreover, we showed that a probabilistic framework for modeling the dependence between environmental variables, such as the copula-based framework proposed here, can provide valuable inputs to propose risk reduction strategies against floods. Specifically, we found that around eastern Hainan Island, where the potential for compound flooding is the highest during typhoon season, surge events are associated with more severe rainfall events. For example, the intensity of rainfall events is about 40.8% higher than the median of annual maxima rainfall (Sun



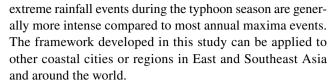
et al. 2021). We also found that in the Bohai Sea area where the majority of extreme events occur during the extra-tropical storm season, the intensity of rainfall events associated with extreme surge conditions has a median value smaller than the median of annual maxima events (88 mm/day). This implies that the severity of the expected rainfall event in case of a storm surge peak is smaller compared to the expected severity inferred from the probability distribution of annual maxima precipitation.

From a design perspective, such a result calls for a more in-depth and case-specific understanding of the interaction between surge and rainfall and an evaluation of which strategy (dependent model versus independent model) for assessing design values is the most appropriate to avoid under-preparedness. For example, the sensitivity of the river to backwater effects can lead to pluvial flooding even for moderate rainfall events hence additional flood protection measures along riverbanks or within the city should be considered. Moreover, the implementation of rainwater storage and hydrograph peak reduction facilities (that is, detention basins) can strengthen the coastal flood protection system's capabilities and enhance the safety of the city (Ke et al. 2018; Najafi et al. 2021), especially when it is expected that surges are associated with higher than expected rainfall, such as along the southern coast of China. It is important, however, to consider that effective water discharges are influenced by several hydrological factors, including topography, land use, soil type, and vegetation cover and neglecting such factors might lead to a misrepresentation of flood risk. More in-depth and case-specific investigations can, for example, be performed via hydrodynamic models that explicitly simulate the interaction between rainfall events and surge conditions.

6 Conclusion

In this study, we proposed a copula-based framework to quantify flood hazards in coastal regions that are exposed to the combination of storm surge and pluvial flooding. This can provide insights into adaptation strategies that account for coastal and pluvial flooding protection infrastructure. We observed that in southern China the highest number of extreme surge events occur during typhoon seasons, while in the northern part of the country the majority of the surge peaks occur during the non-typhoon season. This is expected because typhoons largely affect the southern region.

Our main results are that: (1) There is a positive and significant correlation between surge peaks and rainfall in 10 of the 26 catchments investigated; (2) The probability of rainfall conditional on a specific surge event can provide valuable information for the design of flood protection systems in estuary regions; (3) In southern China (Hainan Island),



One of the main limitations of this study is the relatively small number of tide gauge sites and the 36 years of data available, especially during typhoons. There is an urgent need for longer datasets to be used in order to better assess compound flood risk, especially for southeastern China coasts, which are prone to typhoons. Therefore, monitoring and prediction of rainfall, storm surge, and sea level rise should be an important component of the development of future adaptation and flood management.

Acknowledgments This work is sponsored by the Major Program of National Social Science Foundation of China (Grant No. 18ZDA105), and the National Natural Science Foundation of China (Grant No. 41971199). Jinkai Tan is thankful for financial support from the China Postdoctoral Science Foundation (Grant No. 2021M693584). Hanqing Xu is thankful for financial support from the program of China Scholarships Council (Grant No. 202006140040).

Open Access This article is licensed under a Creative Commons Attribution 4.0 International License, which permits use, sharing, adaptation, distribution and reproduction in any medium or format, as long as you give appropriate credit to the original author(s) and the source, provide a link to the Creative Commons licence, and indicate if changes were made. The images or other third party material in this article are included in the article's Creative Commons licence, unless indicated otherwise in a credit line to the material. If material is not included in the article's Creative Commons licence and your intended use is not permitted by statutory regulation or exceeds the permitted use, you will need to obtain permission directly from the copyright holder. To view a copy of this licence, visit https://creativecommons.org/licenses/by/4.0/.

References

Antonini, A., A. Raby, J.M.W. Brownjohn, A. Pappas, and D. D'Ayala. 2019. Survivability assessment of Fastnet lighthouse. *Coastal Engineering* 150: 18–38.

Bevacqua, E., D. Maraun, I. Hobæk Haff, M. Widmann, and M. Vrac. 2017. Multivariate statistical modelling of compound events via pair-copula constructions: Analysis of floods in Ravenna (Italy). *Hydrology and Earth System Sciences* 21(6): 2701–2723.

Bevacqua, E., D. Maraun, M.I. Vousdoukas, E. Voukouvalas, M. Vrac, L. Mentaschi, and M. Widmann. 2019. Higher probability of compound flooding from precipitation and storm surge in Europe under anthropogenic climate change. *Science Advances* 5(9): eaaw5531.

Bevacqua, E., M.I. Vousdoukas, T.G. Shepherd, and M. Vrac. 2020. Brief communication: the role of using precipitation or river discharge data when assessing global coastal compound flooding. *Natural Hazards and Earth System Sciences* 20(6): 1765–1782.

Burnham, K.P., and D.R. Anderson. 2004. Multimodel inference: understanding AIC and BIC in model selection. *Sociological Methods & Research* 33(2): 261–304.

Coles, S., J. Bawa, L. Trenner, and P. Dorazio. 2001. An introduction to statistical modeling of extreme values. London: Springer.



- Couasnon, A., D. Eilander, S. Muis, T.I. Veldkamp, I.D. Haigh, T. Wahl, and P.J. Ward. 2020. Measuring compound flood potential from river discharge and storm surge extremes at the global scale. Natural Hazards and Earth System Sciences 20(2): 489–504.
- Day, J.A., I. Fung, and W. Liu. 2018. Changing character of rainfall in eastern China, 1951–2007. Proceedings of the National Academy of Sciences 115(9): 2016–2021.
- De Michele, C., and G. Salvadori. 2003. A generalized Pareto intensity-duration model of storm rainfall exploiting 2-copulas. *Journal of Geophysical Research: Atmospheres*. https://doi.org/10.1029/2002ID002534
- Fang, W., X. Zhong, and X. Shi. 2016. Typhoon disasters in China. In Natural disasters in China, ed. P. Shi, 103–131. Berlin: Springer.
- Fang, J., T. Wahl, J. Fang, X. Sun, F. Kong, and M. Liu. 2021. Compound flood potential from storm surge and heavy precipitation in coastal China: dependence, drivers, and impacts. *Hydrology and Earth System Sciences* 25(8): 4403–4416.
- Fang, J., T. Wahl, Q. Zhang, S. Muis, P. Hu, J. Fang, S. Du, T. Dou, and P. Shi. 2021. Extreme sea levels along coastal China: uncertainties and implications. *Stochastic Environmental Research and Risk Assessment* 35: 405–418.
- Feng, J., D. Li, Y. Li, Q. Liu, and A. Wang. 2018. Storm surge variation along the coast of the Bohai Sea. *Scientific Reports* 8(1): 1–10.
- Ghanbari, M., M. Arabi, S.C. Kao, J. Obeysekera, and W. Sweet. 2021. Climate change and changes in compound coastal-riverine flooding hazard along the US coasts. *Earth's Future* 9(5): e2021EF002055.
- Hauke, J., and T. Kossowski. 2011. Comparison of values of Pearson's and Spearman's correlation coefficient on the same sets of data. *Quaestiones Geographicae* 30(2): 87–93.
- Ke, Q., S.N. Jonkman, P.H. Van Gelder, and J.D. Bricker. 2018. Frequency analysis of storm-surge-induced flooding for the Huangpu river in Shanghai, China. *Journal of Marine Science and Engineering* 6(2): 70.
- Kossin, J.P. 2018. A global slowdown of tropical-cyclone translation speed. *Nature* 558(7708): 104–107.
- Lehner, B., Verdin, K., and Jarvis, A. 2008. New global hydrography derived from spaceborne elevation data. Eos, *Transactions*, *American Geophysical Union* 89(10): 93–94. https://doi.org/10.1029/2008eo100001.
- Liu, Q., H. Xu, and J. Wang. 2022. Assessing tropical cyclone compound flood risk using hydrodynamic modelling: a case study in Haikou City, China. *Natural Hazards and Earth System Sciences* 22(2): 665–675.
- Mori, N., T. Shimura, K. Yoshida, R. Mizuta, Y. Okada, M. Fujita, and E. Nakakita. 2019. Future changes in extreme storm surges based on mega-ensemble projection using 60-km resolution atmospheric global circulation model. *Coastal Engineering Journal* 61(3): 295–307
- Muis, S., M. Verlaan, H.C. Winsemius, J.C. Aerts, and P.J. Ward. 2016.
 A global reanalysis of storm surges and extreme sea levels. *Nature Communications* 7(1): 1–12.
- Muis, S., M. Verlaan, R.J. Nicholls, S. Brown, J. Hinkel, D. Lincke, and P.J. Ward. 2017. A comparison of two global datasets of extreme sea levels and resulting flood exposure. *Earth's Future* 5(4): 379–392.
- Najafi, M.R., Y. Zhang, and N. Martyn. 2021. A flood risk assessment framework for interdependent infrastructure systems in coastal environments. Sustainable Cities and Society 64: 102516.
- Pickands III, J. 1975. Statistical inference using extreme order statistics. *The Annals of Statistics* 3(1): 119–131.
- Sadegh, M., H. Moftakhari, H.V. Gupta, E. Ragno, O. Mazdiyasni, B. Sanders, and A. AghaKouchak. 2018. Multihazard scenarios for analysis of compound extreme events. *Geophysical Research Letters* 45(11): 5470–5480.

- Saleh, F., V. Ramaswamy, Y. Wang, N. Georgas, A. Blumberg, and J. Pullen. 2017. A multi-scale ensemble-based framework for forecasting compound coastal-riverine flooding: the Hackensack-Passaic watershed and Newark Bay. Advances in Water Resources 110: 371–386.
- Salvadori, G., and C. De Michele. 2004. Frequency analysis via copulas: theoretical aspects and applications to hydrological events. *Water Resources Research* 40(12): W12511.
- Shi, X., S. Liu, S. Yang, Q. Liu, J. Tan, and Z. Guo. 2015. Spatial-temporal distribution of storm surge damage in the coastal areas of China. *Natural Hazards* 79(1): 237–247.
- Shi, X., Z. Han, J. Fang, J. Tan, Z. Guo, and Z. Sun. 2020. Assessment and zonation of storm surge hazards in the coastal areas of China. *Natural Hazards* 100(1): 39–48.
- Sklar, A. 1973. Random variables, joint distribution functions, and copulas. *Kybernetika* 9(6): 449–460.
- State Oceanic Administration. 1998. State Oceanic Administration Bulletin of Oceanic Disaster of China in 1997. Beijing: China Ocean Press (in Chinese).
- Sun, X., R. Li, X. Shan, H. Xu, and J. Wang. 2021. Assessment of climate change impacts and urban flood management schemes in central Shanghai. *International Journal of Disaster Risk Reduc*tion 65: 102563.
- Vousdoukas, M.I., L. Mentaschi, E. Voukouvalas, A. Bianchi, F. Dottori, and L. Feyen. 2018. Climatic and socioeconomic controls of future coastal flood risk in Europe. *Nature Climate Change* 8(9): 776–780.
- Wahl, T., S. Jain, J. Bender, S.D. Meyers, and M.E. Luther. 2015. Increasing risk of compound flooding from storm surge and rainfall for major US cities. *Nature Climate Change* 5(12): 1093–1097.
- Wang, Q., Y. Xu, N. Wei, S. Wang, and H. Hu. 2019. Forecast and service performance on rapidly intensification process of Typhoons Rammasun (2014) and Hato (2017). *Tropical Cyclone Research and Review* 8(1): 18–26.
- Ward, P.J., A. Couasnon, D. Eilander, I.D. Haigh, A. Hendry, S. Muis, and T. Wahl. 2018. Dependence between high sea-level and high river discharge increases flood hazard in global deltas and estuaries. *Environmental Research Letters* 13(8): 084012.
- Wu, W., S. Westra, and M. Leonard. 2021. Estimating the probability of compound floods in estuarine regions. *Hydrology and Earth System Sciences* 25(5): 2821–2841.
- Xiang, C., L. Wu, and N. Qin. 2021. Characteristics of extreme rainfall and rainbands evolution of super Typhoon Lekima (2019) during its landfall. Frontiers of Earth Science 16: 64–74.
- Zhang, H., W. Cheng, X. Qiu, X. Feng, and W. Gong. 2017. Tide-surge interaction along the east coast of the Leizhou Peninsula, South China Sea. *Continental Shelf Research* 142: 32–49.
- Zheng, F., S. Westra, and S.A. Sisson. 2013. Quantifying the dependence between extreme rainfall and storm surge in the coastal zone. *Journal of Hydrology* 505: 172–187.

